Synthesis of Functionalized Biochar for Phosphate Recovery from Eutrophic Water and its Subsequent Utilization as a P-based Fertilizer for Plant Growth

By

Talha Zubair (2019-NUST-SCEE-BE-Env-301386)

Syed Kumail Abbas (2019-NUST-SCEE-BE-Env-290312)

M. Mudassar Hassan (2019-NUST-SCEE-BE-Env-292691)

Submitted in Partial Fulfilment of the Requirement for the Degree of

Bachelors

In Environmental Engineering

Institute of Environmental Sciences and Engineering

School of Civil and Environmental Engineering

National University of Sciences and Technology

June 2023

Approval Sheet

This is to certify that the thesis titled "Synthesis of Functionalized Biochar for Phosphate Recovery from Eutrophic Water and its Subsequent Utilization as a P-based Fertilizer for Plant Growth" submitted by Mr. Talha Zubair, Mr. Syed Kumail Abbas, and Mr. M. Mudassar Hassan has met the necessary criteria to fulfil the requirements for the degree of Bachelor of Environmental Engineering.

Supervisor: 27/07/2023

Dr. Muhammad Ali Inam

IESE, SCEE, NUST

02/08/23

Dr. Zeeshan Ali Khan

Associate Professor (Head of Department)

IESE, SCEE, NUST

02/08/2023

Dr. Imran Hashmi Professor (Associate Dean)

IESE, SCEE, NUST

Acknowledgement

We extend our utmost appreciation to our supervisor, Dr. Muhammad Ali Inam, for his invaluable guidance, unwavering support, astute observations, and pragmatic counsel, all of which have significantly contributed to the successful completion of our final year project. The individual's extensive experience, extensive knowledge, and professional expertise in the field of water and wastewater treatment have greatly contributed to the successful completion of our final year project. We express our deep gratitude to our families for their steadfast support, nurturing, and solicitude throughout this period. We would like to extend our heartfelt gratitude to Engr. Iqra Irfan, Engr. Uzair Ahmed, and Engr. Waqas Saleem for their invaluable assistance and guidance throughout our project. Their continuous support and provision of relevant resources have been instrumental in our progress. In addition, we express our gratitude to the esteemed Staff Members of IESE for generously granting us access to their facilities to conduct our experimental research.

Abstract

The excess in release of phosphates into aquatic ecosystems from various human sources has caused widespread eutrophication creating significant environmental challenges. In response to this issue, our study aims to address it by developing a new approach to recover phosphates from eutrophic water through the use of functionalized biochar. This recovered phosphate can then be utilized as a fertilizer for plant growth. Our method involves modifying biochar derived from sugarcane bagasse with specific functional groups capable of capturing and retaining phosphate ions efficiently. To analyze the characteristics of the modified biochar, we employed scanning electron microscopy, X-ray diffraction, and Fourier transform infrared spectroscopy techniques. The results demonstrate that using 4 g/L dosage of biochar achieves an optimal adsorption capacity of around 80.25%. By providing a sustainable and integrated approach to phosphate recovery and simultaneously addressing water pollution issues our study offers both an effective solution and a valuable resource for agricultural applications. Incorporating functionalized biochar as a P based fertilizer provides an encouraging avenue for sustainable agriculture practices. By decreasing dependence on conventional chemical fertilizers and addressing concerns related to phosphate pollution it offers an effective solution. Further research could potentially emphasize the optimization of the synthesis process as well as the expansion of production at a larger scale, and find the significant impacts of utilization of bio char on health of soil, its nourishment, and sustainability of ecosystem.

Table of Contents

Introduction 10

1.1 Eutrophication: ..... **Error! Bookmark not defined.**

1.2 Biochar as an adsorbent: ..... **Error! Bookmark not defined.**

1.3 Biochar as a fertilizer: ..... **Error! Bookmark not defined.**

1.4 Iron Activation of Biochar: ..... **Error! Bookmark not defined.**

1.5 Novel Method and Iron Activation: ..... **Error! Bookmark not defined.**

1.6 Objectives: ..... **Error! Bookmark not defined.**

Literature Review ..... **Error! Bookmark not defined.**

2.1 First Study ..... **Error! Bookmark not defined.**

2.2 Second Study ..... **Error! Bookmark not defined.**

2.3 Third Study ..... **Error! Bookmark not defined.**

2.4 Fourth Study 10

Methodology 14

3.1 Preparation of SBC ..... **Error! Bookmark not defined.**

3.1.1 Collection of raw material ..... **Error! Bookmark not defined.**

3.1.2 Sorting and cleaning ..... **Error! Bookmark not defined.**

3.1.3 Drying ..... **Error! Bookmark not defined.**

3.1.4 Grinding ..... **Error! Bookmark not defined.**

3.1.5 Sieving ..... **Error! Bookmark not defined.**

3.1.6 Chemical treatment ..... **Error! Bookmark not defined.**

3.1.7 Washing ..... **Error! Bookmark not defined.**

3.1.8 Drying ..... **Error! Bookmark not defined.**

3.1.9 Storage ..... **Error! Bookmark not defined.**

3.2 Pyrolysis of sugarcane bagasse: ..... **Error! Bookmark not defined.**

3.2.1 Loading the pyrolysis reactor ..... **Error! Bookmark not defined.**

3.2.2 Purging ..... **Error! Bookmark not defined.**

3.2.3 Pyrolysis ..... **Error! Bookmark not defined.**

3.2.4 Cooling ..... **Error! Bookmark not defined.**

3.2.5 Collection of products ..... **Error! Bookmark not defined.**

3.2.6 Analysis ..... **Error! Bookmark not defined.**

3.3 Conditions for Pyrolysis Reactor: ..... **Error! Bookmark not defined.**

3.3.1 Biochar synthesis involves the following conditions: ..... **Error! Bookmark not defined.**

3.3.2 N_2 purging rates at different stages of the process: ..... **Error! Bookmark not defined.**
3.4 Analysis of the pyrolysis products: ..... **Error! Bookmark not defined.**
3.4.1 First Run ..... **Error! Bookmark not defined.**
3.4.2 Second Run ..... **Error! Bookmark not defined.**
3.5 Activation with Iron: ..... **Error! Bookmark not defined.**
3.6 Methodlogy for P- detect ..... **Error! Bookmark not defined.**
3.7 Characterization: ..... **Error! Bookmark not defined.**
3.7.1 Before Activation: ..... **Error! Bookmark not defined.**
3.7.2 After Activation: ..... **Error! Bookmark not defined.**
3.8 Batch Adsorption Experiments: ..... **Error! Bookmark not defined.**
3.8.1 Biochar Dosage: ..... **Error! Bookmark not defined.**
3.8.2 Phosphates Initial Concentration: ..... **Error! Bookmark not defined.**
3.8.3 pH: ..... **Error! Bookmark not defined.**
3.8.4 Contact time: ..... **Error! Bookmark not defined.**
3.8.5 Temperature: ..... **Error! Bookmark not defined.**
3.8.5 Soil Collection and Preparation: 20
4.1 Batch Adsorption Experiments: ..... **Error! Bookmark not defined.**
4.1.1 Biochar Dosage: ..... **Error! Bookmark not defined.**
4.1.2 pH: ..... **Error! Bookmark not defined.**
4.1.3 Contact Time: ..... **Error! Bookmark not defined.**
4.1.4 Phosphates Initial Concentration: ..... **Error! Bookmark not defined.**
4.1.5 Temperature: ..... **Error! Bookmark not defined.**
4.2 SEM-EDS: 27
4.2.1 For Raw-Bio char: 27
4.2.2 Iron-Bio char: 28
4.3 BET Analysis: 29
4.4 Proximate Analysis: 29
4.5 Modelling of Isotherm Data: 30
4.6 Modelling of Kinetic Data: 31
4.7 Gibs free energy: 33
4.8 Pot Test: 33
4.9 Cost-Benefit Analysis: 33
4.9.1 For Biochar Production: ..... **Error! Bookmark not defined.**

4.9.2 For Rice Straw: ..... **Error! Bookmark not defined.**
5.1 Conclusion: ..... **Error! Bookmark not defined.**
5.2 Recommendations: ..... **Error! Bookmark not defined.**
5.2.1 Treatment of Eutrophic Water: ..... **Error! Bookmark not defined.**
5.2.2 Feasibility of Scale-up of the process: ..... **Error! Bookmark not defined.**
5.2.3 Commercialization: ..... **Error! Bookmark not defined.**

List of Tables

Table 1 Effect of biochar dosages on the performance of iron-functionalized biochar towards phosphate from water ..... Error! Bookmark not defined.
Table 2 pH **25**
Table 3 Contact time **24**
Table 4 PO_4-P **24**
Table 5 Properties of Raw-Biochar and Iron-Biochar **29**
Table 6 Characteristics of Raw Biochar Vs Iron-Biochar ..... Error! Bookmark not defined.
Table 7 Isotherm Data of Freundlich and Langmuir Model **34**
Table 8 Kinetic Data of Pseudo First Order (PFO) and Pseudo Second Order (PSO) **34**
Table 9 Gibs **343**

List of Figures

Fig 1 - Pyrolysis Reactor 17
Fig 2 - Effect of temperature on the removal performance of phosphate 26
Fig 3 - SEM Image of Raw-Biochar x1000 27
Fig 4 - EDS of Raw-Biochar Tabular form 27
Fig 5 - SEM Image of Iron-Biochar x1000 28
Fig 6 - EDS of Iron-Biochar Tabular Form 28
Fig 7 - Graphical representation of Isotherm Data 31
Fig 8 - Graphical Representation of Kinetic Data 32
Fig 9 - Graphical Representation of Gibbs free energy 35
Fig 10 – Pictorial l Representation of Pot Test 35
Figure 11 - Comparison of Root length of Plant before and after activation of Biochar with Iron 35
Figure 12 - Comparison of Shoot length of Plant before and after activation of Biochar with Iron 35

Chapter 1

Introduction

1.1 Eutrophication:

Eutrophication is basically the excess release of nutrients into the water bodies mainly nitrogen and phosphorus which engulfs freshwater ecosystems worldwide with its adverse environmental impacts. The main reason for nutrients particularly phosphorus (P) enrichment is the algae and other aquatic flora. This phenomenon triggers the degradation of water quality and significantly impacts the biodiversity in aquatic ecosystems. Variety of sources, including agricultural runoff, wastewater treatment plants, and various anthropogenic activities, contribute to discharge phosphorus, further worsen the impacts. Thus, there is a great need to devise sustainable and cost-effective strategies to remove nutrients from eutrophic water.

1.2 The utilization of biochar as an adsorbent:

In recent times, biochar has emerged as a captivating adsorbent, exhibiting significant potential in the domain of phosphorus removal from eutrophic water. Bio char is a C-rich substance that is formed through process of pyrolysis, which involves the thermal decomposition of organic matter. This organic matter can include various types of waste, such as agricultural residues, forestry by-products, and municipal solid waste. Its expansive surface area, porosity, and adsorption capacity contribute it to an exceptional performance in combatting eutrophication. Moreover, the production of biochar proves to be a budget-friendly and ecologically sound process, capable of aiding in carbon sequestration, thus reducing the impacts of climate change.

1.3 Biochar as a fertilizer:

The utilization of biochar as a phosphorus-based fertilizer for plant growth has been limited due to its low solubility and restricted phosphorus availability. The effectiveness of biochar as a fertilizer is hindered by its inability to provide soluble phosphorus, which is essential for optimal plant growth and development. As a result, there has been an increasing interest in the development of functionalized biochar as a means to enhance phosphate recovery and enhance its solubility and accessibility as a fertilizer. Functionalized biochar refers to biochar that has been modified with functional groups, including carboxyl, hydroxyl, and amino groups.

1.4 Iron Activation of Biochar:

One of the methods for functionalizing biochar involves activating it with iron. Iron activation involves the activation of iron (Fe) into the biochar structure, thereby heightening its adsorption capacity for phosphorus. Iron activation can be accomplished through diverse methods, including impregnation with iron salts, pyrolysis in the presence of iron-containing precursors, or integrating iron-rich materials during the biochar production process. Iron activation not only improves the phosphorus adsorption capacity of biochar but also introduces catalytic properties that can enhance nutrient transformations in soils thus promoting plant growth.

1.5 Novel Method and Iron Activation:

The primary objective of this study is to synthesize functionalized biochar using a novel approach that involves the activation of iron. The objective is to establish a cost-efficient and ecologically sustainable method that eliminates the requirement for harmful substances. Through the incorporation of iron into the structure of biochar, the functionalized biochar will demonstrate enhanced capabilities in terms of phosphorus adsorption capacity and catalytic properties. The approach described above demonstrates promise in effectively extracting phosphate from eutrophic water and subsequently utilizing the biochar as a phosphorus-based fertilizer to improve plant growth.

1.6 Objectives:

The specific objectives of this study are as follows:

1. Synthesize and characterize iron-functionalized biochar for subsequent phosphorus recovery from water.
2. Evaluate the impact of water parameters on the effectiveness of synthesized biochar for phosphate removal from water.
3. Utilize phosphate-loaded iron-functionalized biochar as a P-based fertilizer for plant growth.

Chapter 2

Literature Review

The literature review holds significant importance in the realm of research, serving as an essential component that establishes the foundation for subsequent inquiries. Additionally, it aids in the acquisition of pertinent data, thereby enabling researchers to carry out their investigations with accuracy and a well-defined focus. The aforementioned articles were subjected to a rigorous examination in order to acquire a comprehensive understanding and collect relevant information for the purpose of this project.

The issue of phosphorus (P) contamination in aquatic environments is a matter of significant concern due to its detrimental effects on both water quality and the overall health of ecosystems. The objective of this literature review is to provide a comprehensive analysis of existing research in the field, specifically focusing on studies that investigate the adsorption of phosphate using modified biochar. This paper provides a summary of four influential studies conducted in this particular field, focusing on their significant findings and the practical implications derived from them.

The initial study examines the adsorption capacity of chitosan-modified sugarcane bagasse biochar with respect to inorganic phosphate ions. This investigation was carried out by Manyashe and Cele in 2022. The experimental findings demonstrated a removal rate of 40.23% at a pH level of 3, while a removal rate of 2.99% was observed at a pH level of 8. The researchers observed that the removal effectiveness was unsatisfactory, even at high pH levels, due to a scarcity of active sites and the existence of competing contaminants. This discovery suggests that, in certain circumstances, the modification of chitosan may not yield enhanced phosphate adsorption. (Manyatshe et al., 2022)

The investigation conducted by Palansooriya and Sarkar (2021) centered on the elimination of phosphate from water. Specifically, the researchers examined the efficacy of Fe (III)-loaded chitosan-biochar composite fibers for this purpose. The maximum adsorption capacities of several composite fibers were determined to be 9.63, 8.56, 16.43, and 19.24 mg P g1. The findings indicate that the adsorption capacity of the chitosan biochar composite could

potentially be enhanced through the incorporation of Fe (III). This implies that these materials could be valuable for the purpose of phosphate removal. (Palansooriya et al., 2021)

The investigation conducted by Yin and Liu (2021) employed computational modeling to examine the process of phosphate adsorption on biochar structures that were modified with Mg/Ca in aqueous solutions. The findings of their study demonstrated that the biochar structure supplemented with calcium exhibited greater efficacy in phosphate absorption compared to the biochar structure supplemented with magnesium. Furthermore, the results of the study indicated that the adsorption of metals was more efficient compared to edge adsorption, highlighting the significance of the modified metal within the biochar framework for the adsorption of H_2PO4. The aforementioned findings shows underlying mechanisms involved in the process of phosphate adsorption on engineered biochar. (Yin et al., 2021)

Choi and Jang (2019) conducted a study titled "Sequestration of phosphorus in water through the utilization of an innovative biochar derived from dairy manure coated with calcium hydroxide." The Ca (OH) $_2$-BC exhibited a maximum removal efficiency of 89%, accompanied by an adsorption capacity of 13.6 mg/g. The biochar coated with calcium hydroxide exhibited superior performance compared to biochar treated with calcium oxide and magnesium oxide. However, the performance of biochar in comparison to FeO and ZnO was found to be inferior. The results of this study indicate that the utilization of calcium hydroxide-treated biochar exhibits significant efficacy in the removal of phosphates from the surrounding ecosystem. (Zhang et al., 2021),

When taken as a whole, the articles reviewed provide a wealth of data on how to create and characterize modified biochar materials for phosphate removal. While potential improvements in phosphate adsorption capacity were shown when iron oxide and calcium were included, limitations in pH-dependent removal for phosphate were observed for chitosan-modified biochar. Calcium hydroxide-coated biochar, unlike other coated biochar materials, shown to be an effective adsorbent with improved elimination capability. These findings provide light on the mechanism of phosphate removal and will inform the development of more efficient and long-lasting techniques for removing phosphate from aqueous solutions in the future. (Zhang et al., 2021)

Chapter 3

Methodology

We pursued the following methodology:

3.1 Sugarcane Bagasse Pre-processing:

3.1.1 Acquisition of primary resources

The sugarcane bagasse was generated by a sugar mill and subsequently transported to a laboratory for subsequent processing.

3.1.2 Sorting and cleaning:

A comprehensive analysis was conducted on the collected bagasse in order to eliminate any undesired substances, including stones, plastics, and metals. Subsequently, a washing procedure was conducted using distilled water in order to eliminate any particulate matter such as dirt and dust.

3.1.3 Desiccation

The bagasse was subjected to thermal treatment and kept in the oven and maintaining a 105°C temperature for a duration of 24 hours, until it reached a state of equilibrium in terms of

weight. The objective of the procedure was to remove any moisture present in the bagasse, as it could potentially affect the subsequent stages of processing.

3.1.4 Process of Grinding

Utilizing grinder present in the laboratory, the desiccated bagasse was pulverized into fine particulates to a certain size.

3.1.5 The process of sieving

It is also known as screening, is a method used to separate particles of different sizes by passing them through a sieve.

The pulverized sugarcane bagasse underwent a sieving process using a sieve mesh with a size of 0.2 mm in order to remove any sizable particles and achieve a consistent particle size distribution.

3.1.6 Chemical treatment

It refers to the application of chemical substances in order to modify or alter the properties of a material or substance.

The bagasse that had been sifted underwent a treatment at a specific concentration. The primary objective of this procedure was to eliminate all impurities and enhance the purity of the bagasse.

3.1.7 Cleansing

After the treatment procedure was complete, it was rinsed thoroughly with distilled water to get rid of any unwanted chemicals.

3.1.8 Drying, Process

The cleaned bagasse was baked at 500 degrees Celsius at a rate of 16 degrees per minute until a constant weight was achieved. The bagasse was dried out since some moisture had remained after the chemical treatment.

3.1.9 The Storing Procedure

Containers were used to keep the processed bagasse at room temperature until it could be used. After undergoing the aforementioned steps, the sugarcane bagasse was ready for use in experiments and analyses.

3.2 Pyrolysis process

The pyrolysis process of sugarcane bagasse will be discussed in this section.

3.2.1 Introduction to the Pyrolysis Reactor Loading Process

The bagasse was introduced into the pyrolysis reactor in powdered form. The reactor was designed to operate within a 500°C temperature range while maintaining a 16 degree Celsius per minute heating rate.

3.2.2 Purging

To mitigate the risk of substrate oxidation, nitrogen gas (N_2) was used to purge the reactor in order to remove any traces of air and eliminate the possibility of air contamination.

3.2.3 Pyrolysis Process

With a heating rate of 16°C per minute, the reactor was heated until it reached the specified temperature of 500°C. The feedstock underwent conversion into biochar, bio oil, and bio gas.

3.2.4 Thermal Dissipation

Following conclusion of the above procedure, the reactor subjected to cooling until it reached the surrounding temperature, while being shielded by a nitrogen gas environment.

3.2.5 Product Collection

The biochar, bio-oil, and synthetic gas generated through the pyrolysis process were individually collected and stored in sealed containers for subsequent utilization.

Following the aforementioned procedures, sugarcane bagasse was pyrolyzed under controlled conditions, which was then utilized for experimental and analytical objectives.

3.3 Criteria for Pyrolysis Reactor:

The biochar synthesis procedure includes the subsequent conditions:

• The synthesis is conducted at a temperature of 500 degrees Celsius.

• The heating rate employed in this study involves a rapid temperature increase of 16°C per minute.

The purging rates of N2 at various stages of the process were examined.

- The introduction of nitrogen gas (N_2) into the reactor occurs at a flow rate of 0.2 liters per minute, and this purging process typically lasts for a duration of 10 to 15 minutes.
- A constant flow of nitrogen gas (N_2) is kept constant at 0.1 liter/min for the duration of the process (three hours).
- Following the pyrolysis process, a purging of N_2 gas is conducted at a rate of 0.5 liters per minute for a duration of 15-20 minutes.

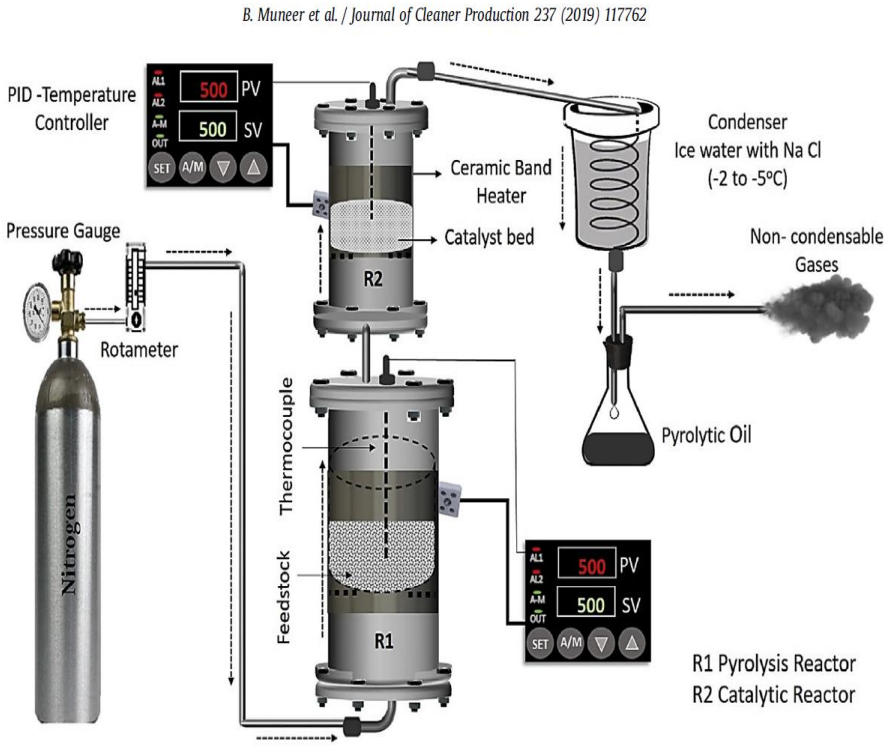

Figure 1 - Pyrolysis Reactor

3.4 Investigation into the pyrolysis byproducts:

3.4.1 Initial Execution

One hundred grams of biomass was used in the first experiment, yielding the following amounts of pyrolysis products:

- The quantity of bio oil under consideration is 38.3 grams.
- The quantity of biochar utilized in the experiment was 49.7 grams.
- The quantity of biogas produced is 12 g.

3.4.2 Subsequent Iteration

A total of 43.6 grams of biomass was added to the reactor in the succeeding experimental session, yielding the aforementioned amounts of pyrolysis products.

- The quantity of bio-oil under consideration is 15.4 grams.
- The quantity of biochar utilized in the experiment was 21.7 grams.
- The biogas sample yielded a mass of 6.5 grams.

Compared to bio-oil, a liquid product, and biogas, a gaseous product, the pyrolysis method produced a greater proportion of biochar, a solid residue. During initial trial, it was observed that 49.77% of the initial biomass underwent a transformation process resulting in the formation of biochar, while 35.3% was converted into bio-oil, and the remaining 14.9% was transformed into biogas. During the second iteration, approximately 49.8% of the biomass underwent a transformation process resulting in the formation of biochar, while 35.4% of the biomass was converted into bio-oil. Additionally, 14.9% of the biomass was transformed into bio gas.

3.5 Iron Activation:

Biochar (10 grams) was added to a 0.1 molar $FeCl_3.6H_2O$ solution. By adding 0.5M NaOH solution, the pH of the solution was adjusted to 11. The solution was heated on a hot plate agitator for 45 minutes at temperature of 60°C. Following the cooling procedure, the solution was filtered, and the pH was neutralized to 7 by adding distilled water. The stable biochar residue was then separated from the liquid by centrifuging the solution.

3.6 Methodology for P-detection:

To execute the procedure, we added 2.5 grams of ammonium molybdate into 30 milliliters of distilled water, followed by 0.125 grams of ammonium metavanadate to an additional 30 milliliters of distilled water. The ammonium metavanadate solution was subjected to heating and subsequent cooling. After this, 33ml of hydrochloric acid (HCl) was added to the ammonium metavanadate-containing solution, and then again cooled. The ammonium molybdate solution was added to the mixture of ammonium metavanadate and hydrochloric acid (HCl) in order to obtain a volume of 100 milliliters. Using the stock solution and the reagents, a calibration curve was finally constructed. It has been proved by researchers that a linear relationship between absorbance and phosphate content was found using the calibration curve.

Ammonium molybdate and ammonium metavanadate were used in an effective and proven method for detecting phosphate. The proposed approach may find use in a wide variety of contexts, such as environmental monitoring and agricultural activities.

3.7 Characterization:

3.7.1 prior to activation:

3.7.1.1 The Scanning Electron Microscopy-Energy Dispersive X-ray Spectroscopy (SEM-EDS) technique:

This method is used to investigate the material's surface morphology or microscopic structure in order to establish its elemental make-up.

3.7.1.2 The BET analysis method:

It is a widely used technique in surface chemistry and materials science. The BET analysis method is employed to quantify the material's specific surface area, porosity, pore size, and pore volume. This provides details regarding the texture and surface properties of the material.

3.7.1.3 The proximate procedure:

The chemical composition of a substance by measuring its various components such as moisture, ash, protein, fat, and carbohydrates can be find by this.

3.7.2 Following the activation process:

3.7.2.1 SEM-EDS:

Using SEM-EDS, the surface morphology and elemental composition of the material following activation are examined in a manner analogous to its condition prior to activation. It facilitates the evaluation of any structural modifications to the material.

3.7.2.2 Brunauer-Emmett-Teller (BET) Analysis (BET analysis)

It measures the surface area, porosity, pore size, and pore volume of the activated material. This facilitates the evaluation of the change in its surface characteristics, and permeability.

3.7.2.3 Proximate Procedure:

It refers to analytical technique used to determine the composition of a substance by examining its various components, such as moisture content, and ash.

3.8.1 Biochar Dosage:

Bio char dosage was varied to check the optimal dosage. The biochar dosage utilized in the experimental study was taken first 0.1grams. A subsequent experiment was conducted utilizing 0.2grams of bio char. Another adsorption experiment in which 0.5gram of biochar was taken. Then, 1gram of biochar was used in the subsequent experimental procedure. The experiment was run

again, this time with twice as much bio char (2gram). Similarly, three grams of bio char were then used in an adsorption experiment. After this, now four grams of bio char were utilized. In the concluding trial of the adsorption test, the biochar dosage of 5grams was used and the results were obtained.

3.8.2 Initial Phosphate Concentration:

The concentration of PO4-P was varied at different levels, specifically 5, 10, 12, 15, 18, and 20 milligrams per liter, in order to determine the optimal initial concentration.

3.8.3 pH:

The experimental study investigated the effect of various pH levels on the adsorption capacity and removal efficiency of biochar (2, 5, 7, and 9).

3.8.4 Contact Period:

To see how changing the contact time affected the adsorption process, we conducted an experiment. We studied time periods of 6mins, 12mins, 30mins, 60mins, and 240mins of interaction. Adsorbate and adsorbent may interact more deeply if given more time to do so during the contact phase. Increases in contact time result in a linear rise in adsorption capacity.

The investigation found that the absorption capacity improved as the contact time went from 0.1 to 4 hours. Nonetheless, it is possible that there exists a threshold beyond which the adsorption capacity does not increase appreciably despite prolonged contact times. It was discovered that the duration of contact between substances had a significant effect on the adsorption capacity, as longer contact periods generally led to greater adsorption capacities.

3.8.5 Temperature:

The temperature measured was 25 degrees Celsius. At a temperature of 35°C, a further experiment was conducted. In the succeeding test, the temperature was increased to 45 degrees Celsius. The experimental investigation consisted of taking 500 mL conical flasks, each of which contained 100 mL of phosphate dosage derived from the initial stock solution. Either, NaOH or HCl was utilized to adjust the pH of the solution. The specimen was treated with varying concentrations of biochar. After attaining the desired temperature, the flask was shaken at a constant rate of 200 revolutions per minute (rpm) using a shaker. Phosphate content was measured

by taking samples at regular intervals and analyzing them using a UV-Vis spectrophotometer set to a wavelength of 470nm.

3.8.5 Soil Collection and preparation:

To carry out this step, we procured soil samples from the NUST nursery near Gate 2. These soil samples were put to a series of processes to ensure the condition for the pot test experiment.

1. Desiccation:

The gathered soil samples were subjected to an oven at 105°C, where all traces of moisture were removed. This dehydration process was of great importance, as it gives us accurate measurements.

2. Pulverization:

Once the soil samples had undergone the important dehydration process, they were subjected to the pounding of a rammer and the grinding of a mortar and pestle. This pulverization process produced uniformity in particle size and facilitated the adsorption with the biochar.

3. Sieving:

The pulverized soil, now free of impurities, was thoroughly sieved through a 2mm mesh sieve, freeing it from any larger particles and ensuring a symmetrical distribution of particle sizes. This process yielded a homogenous soil mixture, aimed for use in the pot test.

Pot Test Arrangement:

Within pots of the pot test, biochar and soil was thoroughly mixed, with a ratio of 2% biochar and 98% soil. Specifically, 1 gram of biochar was mixed with 49 grams of soil. The chosen seed for this experiment was the mustard plant seed (Brassica Juncea).

Root and Shoot Length Observations:

Once the hallowed pot test arrangement was prepared, the mustard plant was nurtured within the mixture of biochar and soil, under controlled conditions. Throughout its growth cycle, the lengths of both its roots and shoots were carefully measured at regular intervals, capturing the whole progression.

Chapter 4

Results and Discussion

4.1 Batch Adsorption Experiments:

4.1.1 Bio char Dosage:

As the biochar dose increased, the adsorption capacity gradually decreased until it reached a critical threshold of 4 g/L, at which time it dropped significantly, yet the removal efficiency increases. The most effective dose for obtaining maximum adsorption capacity, which hovered around 80.25%, was determined to be 4 g/L. Notably, a 5g/L dose resulted in an 81% removal efficiency, although at the price of a substantial decrease in adsorption capacity. As a result, it was ruled inappropriate for use as the recommended dosage.

Table 1- Effect of biochar dosages on the removal performance and adsorption capacity of iron-functionalized biochar towards phosphate from water

Bio-char Dosage (g/L)	Removal Efficiency (%)	Adsorption Capacity (mg/g)
0.1	9.4	9.4
0.2	18.6	9.3
0.5	31.1	6.2
1	52.8	5.2
2	63.6	3.2
3	73.6	2.5
4	80.3	4.5
5	81.1	1.6

4.1.2 pH:

The adsorption capacity decreases as the pH rises; Maximum adsorption capacity observed at acidic pH which performed the best for both adsorption capacity and removal efficacy. At a pH 2, a maximum removal efficacy of 98.5% could be attained. This phenomenon can be attributed to the electrostatic interaction between the surface charge of the biochar and the phosphate ions.

Phosphates exhibit an affinity for biochar within an acidic environment, owing to the activation of biochar facilitated by iron and its inherent positive charge. Therefore, the presence of acidity creates a favorable environment for the process of adsorption.

Table 2- Effect of pH on the removal performance and adsorption capacity of iron-functionalized biochar towards phosphate from water

pH	Removal Efficiency (%)	Adsorption Capacity (mg/g)
2	98.5	2.6
5	91.1	2.3
7	80.3	2
9	67.7	1.7

4.1.3 Contact Time:

The maximum utilization of adsorption capacity was observed as the contact time increased up to 4 hours. However, the outcomes obtained at 2 hours and 4 hours exhibited similar trends. Therefore, the optimal duration for contact was determined to be 2 hours. The occurrence in question arises from the equilibrium state of adsorption, wherein the rate of adsorption is in equilibrium with the rate of desorption.

Table 3- Effect of contact time on the removal performance and adsorption capacity of iron-functionalized biochar towards phosphate from water

Contact Time (HRS)	Removal Efficiency (%)	Adsorption Capacity (mg/g)
0.1	42.7	1.1
0.2	51.8	1.3
0.5	59.5	1.5
1	68.6	1.7
2	80.3	2
4	84.2	2.1

4.1.4 Phosphates Initial Concentration:

The increase in the initial concentration of phosphates in the solution resulted in a corresponding increase in the adsorption capacity. The phenomenon arises from the saturation of adsorption sites on the biochar surface when initial concentrations increase. Conversely, the removal efficacy of 80.25% at an initial phosphate concentration of 5mg/L was observed. The 10mg/l was chosen as the optimal phosphates initial concentration.

Table 4- Effect of PO4-P concentration on the removal performance and adsorption capacity of iron-functionalized biochar towards phosphate from water

PO4-P Concentration (mg/l)	Removal Efficiency (%)	Adsorption Capacity (mg/g)
5	83.2	1.1
10	80.3	2
12	75.8	2.3
15	67.8	2.5
18	62.4	2.8
20	54.4	2

4.1.5 Temperature:

Temperature influences the adsorption process in general, and temperature changes can impact the adsorption capacity. In our experimental investigation, we observed that when the temperature rose to 35°C, the rate of adsorption decreased. The effect of ambient temperature on the rate of adsorption clarifies this phenomenon.

At reduced temperatures, the motion of particles becomes constrained, resulting in a relatively low kinetic energy. The deceleration of adsorbate molecules and their subsequent interaction with the surface of the adsorbent is impeded by this phenomenon. Consequently, the rate of adsorption decelerates, leading to a diminished adsorption capacity.

Nevertheless, as the temperature rises, the kinetic energy exhibited by the molecules will be greater. This increased energy rises the adaptability of the adsorption material molecules, allowing

them to overcome intermolecular interactions and attaches to the adsorbent's surface with greater ease. As a result, at higher temperatures, the rate of adsorption accelerates, resulting in increased adsorption capacity.

The phenomenon can be attributed to the heightened thermal energy leading to desorption or weakened interactions between the adsorbent and adsorbate.

During the course of our empirical investigation, we observed a decline in adsorption capacity beyond a temperature threshold of 35 degree Celsius.

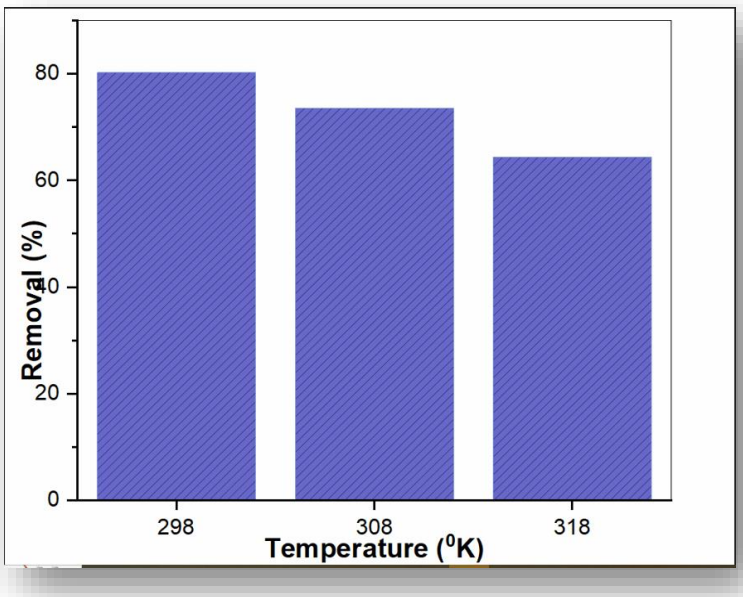

Figure 2 - Effect of temperature on the removal performance of Iron-loaded bio char towards phosphate water

4.2 SEM-EDS:

4.2.1 For Raw Bio char:

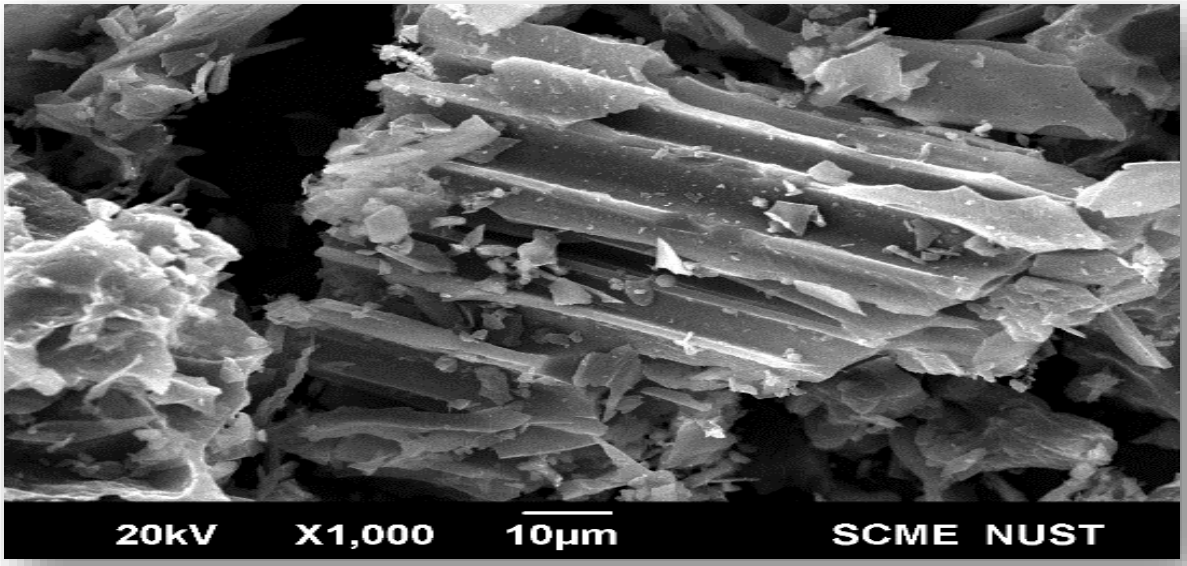

Figure 3 - SEM of Raw Bio char x1000

eZAF Quant Result - Analysis Uncertainty: 14.48 %

Element	Weight %	MDL	Atomic %	Error %
C K	77.1	1.02	85.9	10.0
O K	13.0	0.30	10.9	12.6
Mg K	0.8	0.09	0.5	10.8
P K	3.0	0.08	1.3	3.7
K K	1.4	0.10	0.5	5.3
Cu K	2.5	0.29	0.5	9.0
Zn K	2.2	0.35	0.4	4.8

Figure 4 - EDS of Raw Bio char Tabular form

4.2.2 Iron-Biochar:

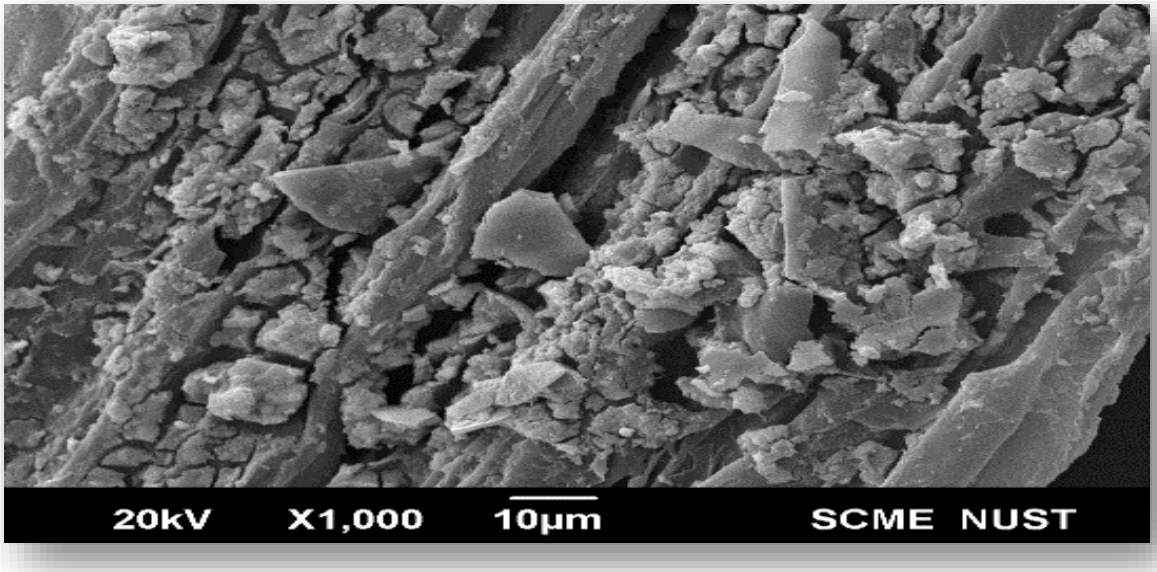

Figure 5 - SEM of Fe Bio char x1000

The results above are of SEM in the form of pictorial representation, employing a specific lens and precision, specifically 10um at 1000X for Raw Biochar and Iron-Loaded Biochar. They exhibit the unorthodox and jagged façade of the two commodities. In the case of the latter, it magnificently displays the interlocking of iron atoms with the biochar molecule.

eZAF Quant Result – Analysis Uncertainty: 11.29 %

Element	Weight %	MDL	Atomic %	Error %
C K	40.7	1.32	59.7	11.0
O K	27.6	0.37	30.4	10.8
K K	0.4	0.13	0.2	18.0
Fe K	27.4	0.28	8.6	2.5
Cu K	2.2	0.42	0.6	16.7
Zn K	1.6	0.50	0.4	6.6

Figure 6 - EDS of Iron-Biochar Tabular Form

The EDS analysis involves quantifying the number of occurrences at various electron beam wavelengths used. Diverse peaks manifest at different wavelengths, which align with the weight percentage of element composition for the pair of products. The element carbon emerges

as the dominant component, exhibiting the highest proportion, as a result of the combination of biochar derived from organic waste materials.

4.3 BET Analysis:

Table 5- Surface Properties of Raw Biochar and Iron-Biochar

Characteristics	**Raw Biochar**	**Iron-Biochar**
Pore volume (cm^3/g)	0.05	1
Pore diameter (nm)	1.7	1.2
Surface area (m^2/g)	31.6	27.2

Sugarcane bagasse bio char demonstrates a narrowing of the pore size distribution throughout the activation process. Iron addition to the outer layer of raw sugarcane bagasse may account for the observed reduction in surface area and pore volume. It is possible that the introduction of iron injection has resulted in the formation of pore blockages within the bio char.

During the process of activation, it is possible to introduce supplementary substances, such as iron, with the intention of modifying the characteristics of the biochar. In this particular scenario, it is possibility that the existence of iron on the surface of the raw sugarcane bagasse (RBC) may have resulted in the obstruction of pores, thereby impeding the internal pore structure.

Consequently, there is a reduction in the surface area available for adsorption. The dimensions and capacity of the pores, which serve as indicators of their size and volume, are reduced due to the effects caused by the presence of iron.

4.4 Proximate Analysis:

Table 6- Properties of Raw Biochar and Iron-Biochar

	Moisture Content	**Volatile Combustible Matter**	**Fixed Carbon**	**Ash Content**
Raw SBC	12.7 %	67.9 %	16.1 %	3.3%
Raw Biochar	7.6 %	49.4 %	40 %	3 %
Fe-Biochar	11.6 %	32.8 %	53.6 %	2 %

The data presented in the table indicates a decrease in volatile combustible matter after the activation, which is resulting in an increase in fixed carbon content.

4.5 Modelling of Isotherm Data:

Table 7- Isotherm Data of Freundlich and Langmuir Model

Model	**Equation**	**Plot**	**K_f**	**N**	**R-Square**
Freundlich	$Q_e=k.C^{1/n}$	Q_e	1.5	3.3	0.956
Langmuir	$Q_e=(q_m.k.C_e)/(1+(k.C_e))$	Q_e	3.2	0.8	0.993

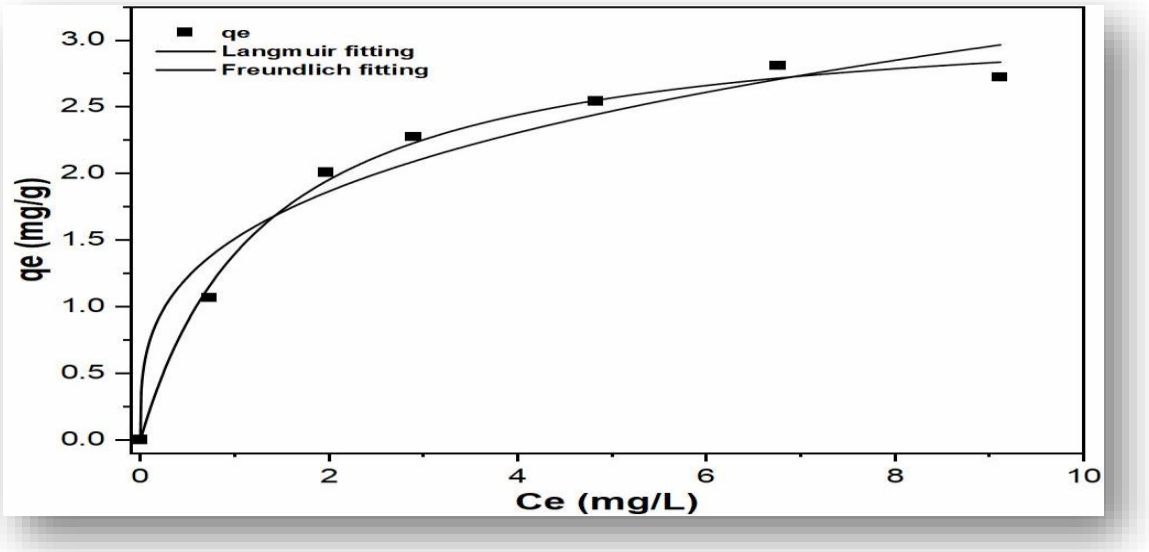

Figure 7 - Graphical representation of Isotherm Data

The adsorption mechanism of biochar is demonstrated through the utilization of isotherm models. The present observation reveals the emergence of two distinct mathematical models, namely the Langmuir and Freundlich curves, which exhibit intriguing characteristics. Nevertheless, this remarkable product exhibits a strong affinity for the Langmuir curve fitting, revealing the impressive capabilities of biochar in monolayer adsorption. As a result, this process enhances the exceptional adsorption capacity of biochar, enabling it to effectively capture phosphate ions in its active sites.

4.6 Modelling of Kinetic Data:

Table 8- Kinetic Data of Pseudo First Order (PFO) and Pseudo Second Order (PSO)

Model	**Equation**	**Plot**	**Q_e**	**K_t**	**R-Square**
PFO	$Q_t=q_e-(\exp((\ln(q_e))-(k.t)))$	Q_t	1.9	2.6	0.9147
PSO	$Q_t=((k.q_e^2.t)/(1+(k.q_e.t)))$	Q_t	2.2	1.6	0.9573

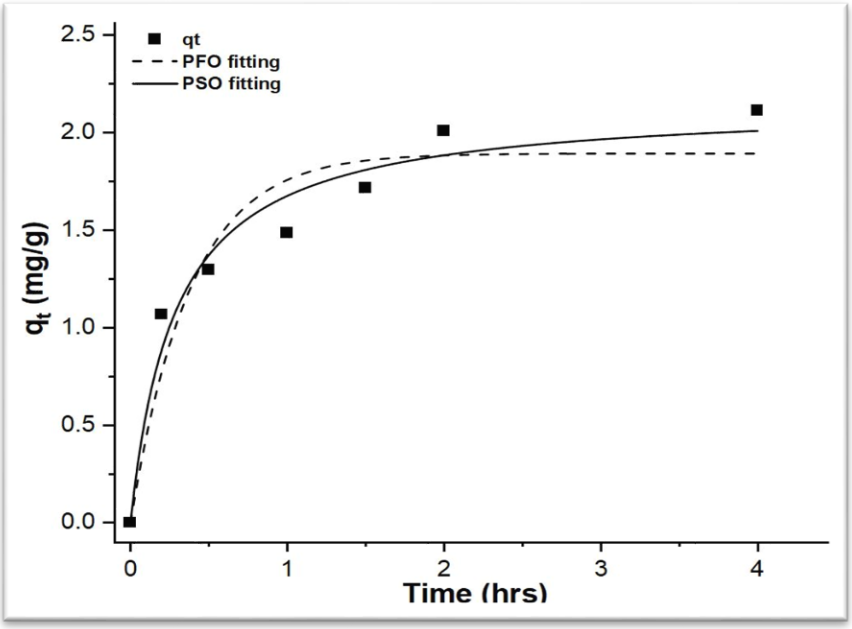

Figure 8 - Graphical Representation of Kinetic Data

Based on the dynamic data illustrated in Table 10, it becomes apparent that the adsorption of the adsorbate onto the iron-activated biochar adheres to the pseudo-second-order (PSO) model. The PSO framework offers a more precise depiction of the adsorption kinetics for this system in comparison to the pseudo-first-order (PFO) model as presented in Table 8.

The PSO model equation, is as follows:

$$Qt = (k.qe^2.t) / (1 + (k.qe.t))$$

Wherein, Q_t represents the quantity of adsorbate assimilated at time t (mg/g), K denotes the constant of the PSO model (g/ (mg·min)), Q_e stands for the equilibrium adsorption capacity (mg/g), T symbolizes the contact time (min).

From Table, the values of qe and k for the PSO model are observed as 2.2 and 1.6, respectively. These values represents the equilibrium adsorption capacity and the constant K for the PSO model. Besides, an adjusted R-squared value of 0.9 signifies a commendable fit of the PSO model to the empirical data.

The PSO model suggests that the rate-controlling step of adsorption on the iron-activated bio char involves a chemical interaction between the adsorbate and the sites on the bio char surface. It is worth mentioning that the PSO model considers the interation between the adsorbate and the biochar surface as a chemisorption process, which aligns with the prevailing activated iron species on the biochar surface.

The graph of qt (quantity of adsorbate assimilated at time t) against time, as depicted in Table, would display a distinctive pattern showed by the PSO model equation. The empirical data for adsorption on the iron-activated biochar can be fitted to this equation, providing insights into the adsorption kinetics and enabling the determination of kinetic parameters.

Overall, the observation that the adsorption of the adsorbate onto the iron-activated biochar adheres to the pseudo-second-order model implies that the chemisorption process encompassing activated iron species on the biochar surface plays a pivotal role in the adsorption mechanism. This discovery carries significant implications for optimizing the efficacy of iron-activated biochar as an adsorbent in a wide range of water and wastewater treatment applications, where the efficient elimination of contaminants is highly desired.

4.7 Gibbs free energy:

The Gibbs free energy provides enlightened insights into the originality and feasibility of our adsorbent activity in the context of our adsorption process. We carried out an adsorption experiment that generated positive outcomes by seeking an exothermic reaction.

Adsorption refers to the phenomenon wherein adsorbate molecules are bound to the surface of an adsorbent material. Diverse intermolecular forces modify the affinity of the adsorbate and adsorbent. We can determine the thermodynamic favorability of the adsorption approach by computing the gibbs free energy change (G).

Our laboratory experiments led us to use the formula G = H - TS. The following are necessary for evaluating the iron-loaded biochar (Fe-BC) adsorption study's data: The slope of the line (b) is 0.10645, indicating a positive connection between adsorption capacity (Y) and adsorbate concentration (x), and the computed value for the intersection of lines (a) is -31.7903.

The data fit the regression model rather well, as shown by the corrected R-squared value of 0.90177. This suggests that adsorption onto the Fe-BC surface is dose-dependent.

Our results imply that the adsorption method we used has thermodynamic benefits, since the adsorption process was exothermic and a clear association was found between adsorption capacity and adsorbate concentration. The Gibbs free energy (G) and the total energy of the system were both reduced following adsorption due to the high affinity the adsorbate molecules showed for the Fe-BC surface.

Table 9- Gibbs free energy

Equation	**Plot**	**Weight**	**Intercept**	**Slope**	**R-Square**
$\Delta G = \Delta H - T\Delta S$	Fe-BC	No Weighting	-31.8	0.1	0.9924

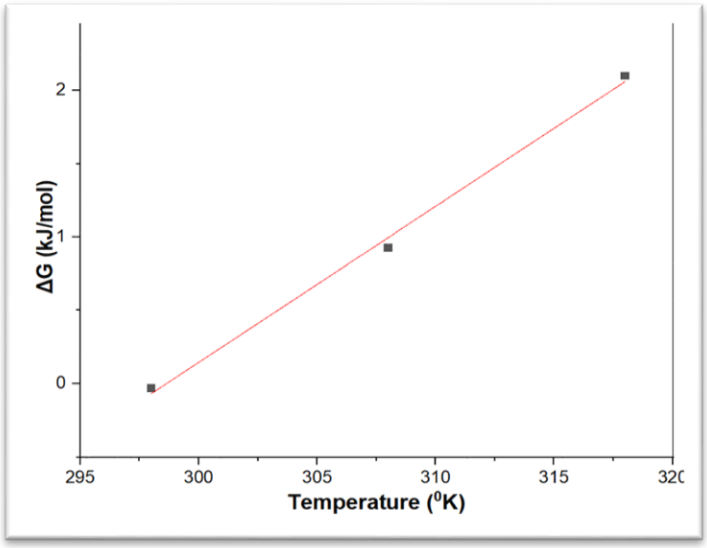

Figure 9 - Graphical Representation of Gibbs free energy

4.8 Pot Test (Phosphate-based fertilizer):

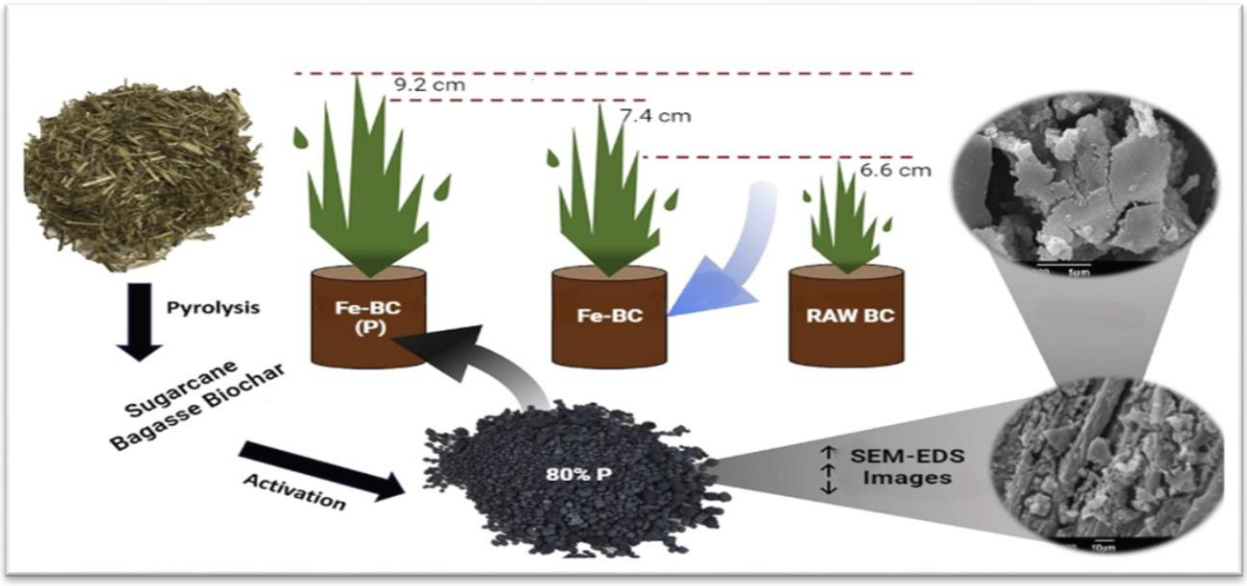

Figure 10 - Pictorial Representation of Pot Test

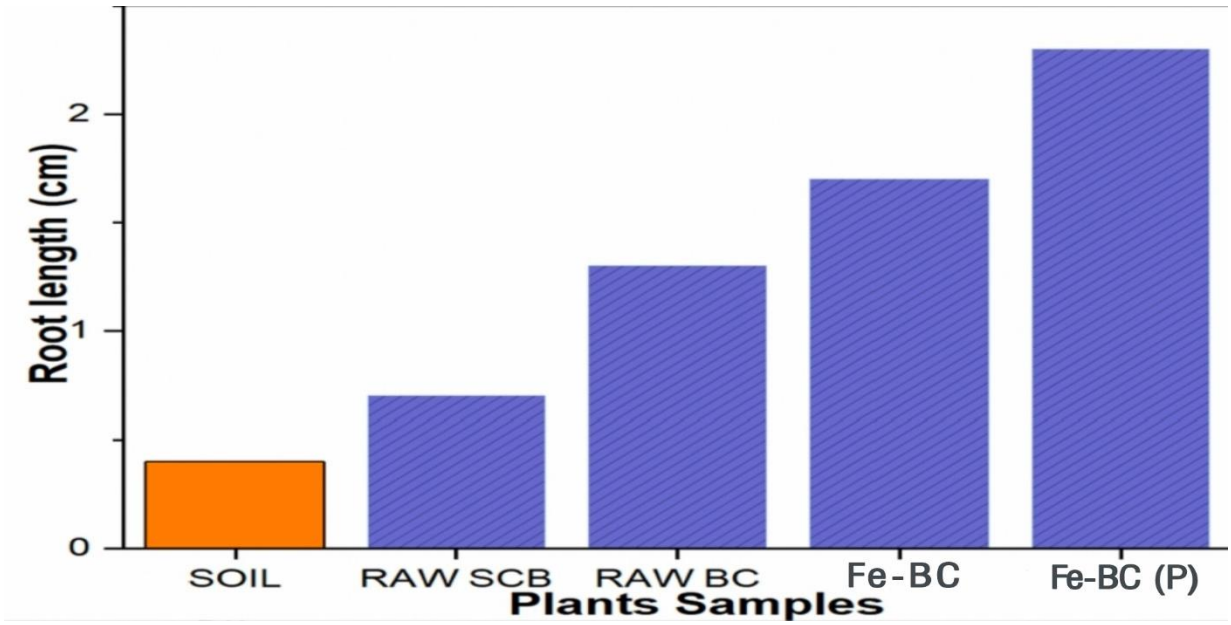

Figure 11 – Comparison of Root length of Plant before and after activation of Biochar with Iron

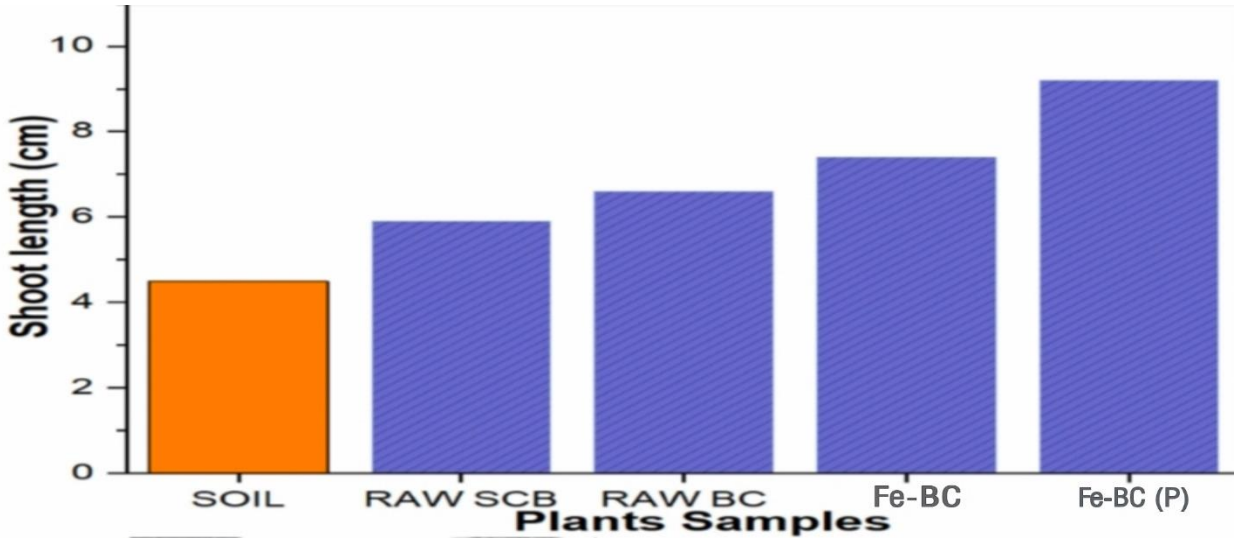

Figure 12 – Comparison of Shoot length of Plant before and after activation of Biochar with Iron

During the phase of data analysis, the measurements of root and shoot lengths derived from the pot test were analyzed to evaluate the impact of bio char addition on the flourishing of plants. We employed statistical techniques, such as mean comparison and t-tests, to ascertain the significance of the outcomes. The analysis revealed that the inclusion of biochar in the soil had a

positive effect on the growth of the mustard plant. Specifically, the root and shoot length increases after the activation of biochar with iron. These findings imply that the activated biochar had advantageous effects on the growth and development of the plants.

The augmented root and shoot lengths observed after the activation of biochar with iron can be ascribed to various factors. The activated bio char potentially enhanced the availability and retention of nutrients in the soil, thus supplying imperative elements for plant growth. Furthermore, it could have fortified the structure of the soil, leading to improved water retention and aeration, which are pivotal for optimal plant growth. The acquired results hold significance as they exhibit the potential of activated bio char as a soil amendment to stimulate plant growth. By elevating the root and shoot lengths, activated bio char might contribute to amplified nutrient absorption, biomass production, and overall plant well-being.

These findings underscore the appropriateness of bio char-amended soil for cultivating plants and propose that the activation of biochar with iron can further boost its positive impacts on plant growth. The utilization of activated biochar as an environmentally friendly and sustainable soil amendment presents promising implications for agricultural practices and endeavors to restore ecosystems. It is crucial to acknowledge that further research and experimentation are recommended to include into the underlying mechanisms and refine the application of activated biochar for different plant species and soil conditions. Nonetheless, the present findings enrich our knowledge of bio char's potential as a valuable approach in sustainable agriculture and land management practices.

4.9 Costs and Benefits Analysis

4.9.1 The process of Bio char Manufacturing

The estimated cost range for biochar production from sugarcane bagasse is between 2,200 and 2,500 PKR per tonne. The costs associated with the collection and transportation of sugarcane bagasse ranges from 800 to 1,500 PKR. The pyrolysis operation costs are in between 1,000 and 1,200 PKR, while the expenses for post-processing and storage amount to 400-800 PKR.

4.9.2 Regarding Rice Straw

In contrast, it has been estimated that the overall cost per metric ton for the production of biochar from rice straw amounts to 3,500 PKR. The aforementioned expenses encompass the expenditures associated with the collection and transportation of rice straw (1,600 PKR), the process of pyrolysis (1,300 PKR), as well as the subsequent activities of post-processing and storage (600 PKR).

According to the research findings, rice straw biochar demonstrates a maximum removal efficiency of 83%. Nonetheless, through the optimization of all parameters, it is anticipated that the utmost efficiency will reach approximately 98.5%.

The value of the advantages gained from using biochar, as well as market demand and possible income from biochar sales, are additional considerations that must be included into a thorough cost-benefit analysis. Increased soil fertility, carbon sequestration, and reduced emissions of greenhouse gases are only some of the possible outcomes of adopting such approaches.

A thorough review of overall expenses and potential earnings will help decision-makers in Pakistan determine whether or not bio char production from sugarcane bagasse and rice chaff is economically viable and profitable. This study's goal is to help people make better decisions by evaluating the practicability and sustainability of the biochar manufacturing method.

CHAPTER 5

Conclusion and Recommendations

5.1 Conclusion

The discoveries of this study reveal that, after optimizing parameters including pH and operating conditions, a remarkable removal efficiency of 80.25% was accomplished under ambient conditions, and at pH 7. This emphasizes the potency of the functionalized biochar in eradicating a substantial portion of the targeted contaminants from water. Furthermore, with the utilization of all optimal parameters, a maximum efficiency of 98.3% could be attained. This outcome shows the tremendous potential of the functionalized biochar when favorable conditions are considered and applied. Additionally, the kinetics of the adsorption process can be better understood by considering the Pseudo second-order reaction model. The results of this study indicate that the process of contaminant adsorption onto biochar that has been loaded with iron can be described by the Langmuir isotherm model. Overall, the findings highlight functionalized bio char's potential as an environmentally feasible and sustainable method for treating eutrophic water and recovering essential nutrients. This emphasizes the broader implications of the study, showcasing the promising capability of functionalized biochar in addressing the challenges associated with excessive nutrient levels in water bodies while potentially enabling the reuse or recycling of valuable extracted nutrients.

5.2 Recommendations

In order to enhance the future development and application of biochar, several recommendations can be put forth.

5.2.1 Treatment of Eutrophic Water:

Actual samples from eutrophic lakes can be analyzed to verify the actual efficiency of the iron-loaded biochar. There will be deviations from the experimental results due to the lack of lab-scale conditions.

5.2.2 The process's ability to be scaled up:

The impressive efficacy of biochar in eradicating various substances necessitates additional investigation into its potential for practical application. Understanding the scalability,

cost-effectiveness, and practical aspects of large-scale production may be gained via the manufacturing process at greater scales. Well the following phase will facilitate the assessment of the suitability of biochar for widespread implementation and integration into existing treatment systems or industrial practices.

5.2.3 Commercialization:

Further investigation into the potential of biochar as a viable and environmentally friendly adsorbent can be conducted by prioritizing the optimization of various parameters, performing comparative analyses, and exploring the feasibility of scaling up production. These endeavors will yield valuable insights that can inform the future application and commercialization of biochar.

References

- Manyatshe , A. et al. (2022) Chitosan modified sugarcane bagasse biochar for the adsorption of inorganic phosphate ions from aqueous solution, Journal of Environmental Chemical Engineering. Available at: https://www.sciencedirect.com/science/article/abs/pii/S2213343722011162

- Palansooriya, K.N. et al. (2021) Fe(III) loaded chitosan-biochar composite fibers for the removal of phosphate from water, Journal of Hazardous Materials. Available at: https://www.sciencedirect.com/science/article/abs/pii/S0304389421004271

- Yin, Q. *et al.* (2021) *Computational study of phosphate adsorption on Mg/Ca modified biochar structure in aqueous solution*, *Chemosphere*. Available at: https://www.sciencedirect.com/science/article/abs/pii/S0045653520335724

- Zhang, X. *et al.* (2021) *Removal of phosphate from aqueous solution by chitosan coated and lanthanum loaded biochar derived from urban dewatered sewage sludge: Adsorption mechanism and application to lab-scale columns*, *Water Science and Technology*. Available at: https://iwaponline.com/wst/article/84/12/3891/85118/Removal-of-phosphate-from-aqueous-solution-by

- Yong-Keun Choi, Hyun Min Jang, Eun-Sung Kan. "Adsorption of phosphate in water on a novel calcium hydroxide-coated dairy manure-derived biochar." Environmental Engineering Research, vol. 24, no. 3, 2019, pp. 434-442.

- Kumar Vikrant, Ki-Hyun Kim, Yong Sik Ok. "Engineered/designer biochar for the removal of phosphate in water and wastewater." Science of The Total Environment, vol. 616–617, March 2018, pp. 1242-1260.

- National Aquatic Resource Surveys. "Indicators: Phosphorus?" [online] Available at: https://www.epa.gov/national-aquatic-resource-surveys/indicators-phosphorus

UG_12 FYDP

ORIGINALITY REPORT

11%	9%	7%	6%
SIMILARITY INDEX	INTERNET SOURCES	PUBLICATIONS	STUDENT PAPERS

PRIMARY SOURCES

1	www.researchgate.net Internet Source	1%
2	Submitted to Binus University International Student Paper	1%
3	repository.upi.edu Internet Source	1%
4	Submitted to University of Northumbria at Newcastle Student Paper	1%
5	Submitted to University of South Australia Student Paper	<1%
6	Submitted to Midlands State University Student Paper	<1%
7	Submitted to University of Bedfordshire Student Paper	<1%
8	link.springer.com Internet Source	<1%
9	www.science.gov Internet Source	<1%

10	Submitted to University of Arizona Student Paper	<1 %
11	Submitted to University of Bradford Student Paper	<1 %
12	www.nature.com Internet Source	<1 %
13	Submitted to University of Wales central institutions Student Paper	<1 %
14	sdhrc.bums.ac.ir Internet Source	<1 %
15	Submitted to University of KwaZulu-Natal Student Paper	<1 %
16	coek.info Internet Source	<1 %
17	Fatemeh Yazdi, Mansoor Anbia, Mohammad Sepehrian. "Recent advances in removal of inorganic anions from water by chitosan-based composites: A comprehensive review", Carbohydrate Polymers, 2023 Publication	<1 %
18	Submitted to University of Venda Student Paper	<1 %
19	Eun Woo Shin, James S. Han, Min Jang, Soo-Hong Min, Jae Kwang Park, Roger M. Rowell.	<1 %

	"Phosphate Adsorption on Aluminum-Impregnated Mesoporous Silicates: Surface Structure and Behavior of Adsorbents", Environmental Science & Technology, 2004 Publication	
20	P. Bhattacharyya, J. Bisen, D. Bhaduri, S. Priyadarsini et al. "Turn the wheel from waste to wealth: Economic and environmental gain of sustainable rice straw management practices over field burning in reference to India", Science of The Total Environment, 2021 Publication	<1 %
21	www.mdpi.com Internet Source	<1 %
22	Submitted to Waterford Institute of Technology Student Paper	<1 %
23	bwcbesant.in Internet Source	<1 %
24	M. Ali Akbar, Farah Aini Abdullah, Mst. Munny Khatun. "Comprehensive geometric-shaped soliton solutions of the fractional regularized long wave equation in ocean engineering", Alexandria Engineering Journal, 2023 Publication	<1 %
25	Submitted to Universiti Sains Malaysia Student Paper	<1 %

26	Mengxue Li, Tianhu Chen, Haibo Liu, Xuehua Zou, Lanbao Zhu, Li Ma, Jing Wang, Yan Ding. "Spectroscopic and Surface Complexation Modeling of Phosphate Enrichment on Porous Iron-Carbon Composites", Water, Air, & Soil Pollution, 2023 Publication	<1 %
27	S Babel. "Low-cost adsorbents for heavy metals uptake from contaminated water: a review", Journal of Hazardous Materials, 2003 Publication	<1 %
28	Shuning Qin, Haodong Fan, Li Jia, Yan Jin, Zepeng Li, Baoguo Fan. "Molecular Structure Analysis and Mercury Adsorption Mechanism of Iron-Based Modified Biochar", Energy & Fuels, 2022 Publication	<1 %
29	bioresources.cnr.ncsu.edu Internet Source	<1 %
30	digital.lib.usf.edu Internet Source	<1 %
31	etd.aau.edu.et Internet Source	<1 %
32	harvest.usask.ca Internet Source	<1 %
33	iwaponline.com Internet Source	

		<1%
34	s3-us-west-2.amazonaws.com Internet Source	<1%
35	www.eeer.org Internet Source	<1%
36	www.freepatentsonline.com Internet Source	<1%
37	Ashwani Kumar Sahu, Indra Deo Mall, Vimal Chandra Srivastava. "STUDIES ON THE ADSORPTION OF FURFURAL FROM AQUEOUS SOLUTION ONTO LOW-COST BAGASSE FLY ASH", Chemical Engineering Communications, 2007 Publication	<1%
38	Submitted to Middlesex University Student Paper	<1%
39	Ramlah Abd Rashid, Ali H. Jawad, Mohd Azlan Mohd Ishak, Nur Nasulhah Kasim. "KOH-activated carbon developed from biomass waste: adsorption equilibrium, kinetic and thermodynamic studies for Methylene blue uptake", Desalination and Water Treatment, 2016 Publication	<1%

40	Sulin Xiang, Minghang Chu, Congyuan Gong, Biaoliang Fang. "Adsorption Performance and Mechanism of Phosphate in Water by Magnesium Oxide-Corncob Biochar", Journal of Environmental Engineering, 2023 Publication	<1 %
41	eprints.polsri.ac.id Internet Source	<1 %
42	mdpi-res.com Internet Source	<1 %
43	qspace.qu.edu.qa Internet Source	<1 %
44	research.library.mun.ca Internet Source	<1 %
45	www.admaterials.com Internet Source	<1 %
46	www.hindawi.com Internet Source	<1 %
47	www.ukm.my Internet Source	<1 %
48	Meenakshi, S.. "Identification of selective ion-exchange resin for fluoride sorption", Journal of Colloid And Interface Science, 20070415 Publication	<1 %

Exclude quotes	Off	Exclude matches	Off
Exclude bibliography	On		